J. Opt. Commun. 19 (1998) 2, 54–60

Journal of Optical Communications

Transmission Characteristics of Single-mode Graded Index Fibers Based on Spot Size Calculations

Moustafa H. Aly, M. Sami A. Abouelwafa, Mohamed M. Keshk

Summary

In this paper, a quantitative estimation of some important transmission characteristics of single-mode graded index fibers is reported at the 1.3 μm and 1.55 μm wavelength windows. The wave equation is solved to get the near-field in the form of a Kummer function. Two spot sizes, W_p and W_{rms} are calculated at different fiber parameters by a numerical integration for the near-field. The accuracy of the method used is tested by a comparison with the power series solution, where a fair agreement for both spot sizes is obtained. Based on the calculated spot sizes, the transmission characteristics are estimated including splice, bending and microbending losses and the chromatic dispersion.

1 Introduction

In the last few years most of the research interests in optical fibers have shifted to single-mode fibers [1]. Single-mode optical fibers are most suitable for high-data-rate transmission systems because of the absence of intermodal dispersion. They can maintain a state of polarization over long lengths [2]. For this reason, they are desirable for use in coherent optical communications. Single-mode fibers are also capable of transmitting power in only one polarization state and they have also a great advantage in interconnecting fibers and polarization-sensitive devices [3].

One of the most important parameters characterizing a single-mode fiber is its modal field from which one can determine various propagation characteristics such as dispersion, source to fiber coupling, splice loss, microbending loss, etc. [4]. All these characteristics could be determined in terms of the so called spot size. The spot size is essentially a representation of the spatial width of the LP_{01} mode field. Till recently, it appeared that a unique definition for the spot size (the distance between the opposite 1/e field amplitude points) would be sufficient to characterize dimensionally a single-mode fiber [5]. Now, two types of spot sizes have been found; W_p, the Petermann spot size, which is proportional to the inverse of the rms half width of the far field angular intensity distribution of the LP_{01} mode [4] and W_{rms} the rms spot size of the near field. Both spot sizes are most commonly used to study all the quantities of interest for a single-mode fiber.

The main reason of evaluating the spot sizes is to study the pulse dispersion and the fiber extrinsic losses as functions of fiber parameters. For single-mode step index fibers, both spot sizes have been estimated from the far-field measurement by B. P. Pal et al. [4] and have also been computed analytically by B. P. Pal et al. [6].

In the present study, the analytical solutions for a graded index (parabolic profile) fiber are utilized to obtain the modal field in the form of Kummer function [7] and consequently the two spot sizes are obtained. A power-series solution is also used to check the accuracy of the analytical one. Transmission characteristics for this fiber are then studied including chromatic dispersion and extrinsic losses; namely, splice loss [8], bending loss [9] and microbending loss [10, 11].

2 Theory

The fiber under consideration is characterized by a graded refractive index profile, n(R), of the form:

$$n^2(R) = n_1^2[1 - 2\Delta f(R)], \quad R \le 1 \qquad (1\,a)$$

$$n^2(R) = n_1^2[1 - 2\Delta], \quad R \ge 1 \qquad (1\,b)$$

where Δ is a grading parameter and $f(R) = R^2$ for a parabolic profile, where R(= r/a) is the normalized radial distance and a is the core radius.

Given the refractive index profile, it is possible to find the near-field pattern, F(R), by solving the wave equation. In the present study, we are limited to single-mode

Address of authors:

Engineering Mathematics and Physics Department
Faculty of Engineering
University of Alexandria
Alexandria, 21544, Egypt

Received 15 July 1996

operation and the wave equation is written in the form [12]:

$$\left[\frac{d^2}{dR^2}+\frac{1}{R}\frac{d}{dR}+\left\{U^2-V^2f(R)\right\}\right]F(R)=0, \tag{2}$$

where V is the normalized frequency and U is the core eigen value given by:

$$V=ka\left(n_1^2-n_2^2\right)^{1/2}, \tag{3 a}$$

$$U^2=a^2\left(n_1^2k^2-\beta^2\right), \tag{3 b}$$

where k (=$2\pi/\lambda$) is the wave number, λ is the free space wavelength, n_1, n_2 are respectively the axial and cladding refractive indices and β is the propagation constant.

2.1 Kummer function solution

The analytical solutions of (2), corresponding to the fundamental mode, LP_{01}, in the core and cladding, respectively, are [13]:

$$F(R)=\exp\left(-0.5VR^2\right).\ M\left[\frac{1}{2}-\frac{U^2}{4V},1,VR^2\right],$$

$$0\le R\le 1 \tag{4 a}$$

$$F(R)=\exp(0.5).\ M\left[\frac{1}{2}-\frac{U^2}{4V},1,V\right]\frac{K_0(WR)}{K_0(W)},$$

$$R\ge 1 \tag{4 b}$$

where M [a,b,z] is the Kummer function, $K_n(x)$ is the modified Bessel function and W is the cladding eigen value, given by:

$$W^2=a^2\left(\beta^2-n_2^2k^2\right)=V^2-U^2. \tag{5}$$

The propagation constant, β, can be calculated from the characteristic equation obtained by matching the field first derivatives at the core-cladding interface. Using (4 a) and (4 b) one can get the characteristic equation as:

$$2V\left\{AM[A+1,2,V]-0.5M[A,1,V]\right\}=$$
$$-W\frac{K_1(W)}{K_0(W)}M[A,1,V], \tag{6}$$

with $A=0.5-U^2/4V$.

2.2 Power series solution

To check the accuracy of Kummer function solution, a power series solution for the parabolic profile is adopted. In the core region, (2) has a power-series solution for the fundamental mode of the form [9]:

$$F(R)=\frac{\sum_{n=0}^{\infty}a_nR^n}{\sum_{n=0}^{\infty}a_n},\quad 0\le R\le 1 \tag{7 a}$$

where a_n are the series coefficients.

In the cladding region, the solution is the zero order modified Bessel function of the second kind, given by [14]:

$$F(R)=\frac{K_0(WR)}{K_0(W)},\quad 1\le R\le\infty \tag{7 b}$$

2.3 Spot size calculations

Once the modal field, F(R), for a particular index profile is determined, one can obtain the two spot size types W_{rms} and W_p which are directly defined from F(R) through [4]:

$$W_{rms}^2=\frac{2a^2\int_0^{\infty}R^3F^2(R)dR}{\int_0^{\infty}RF^2(R)dR}, \tag{8}$$

$$W_p^2=\frac{2a^2\int_0^{\infty}RF^2(R)dR}{\int_0^{\infty}\frac{dF(R)}{dR}RdR}. \tag{9}$$

2.4 Extrinsic losses

2.4.1 Splice loss

Splice losses may occur due to three major defects: longitudinal separation, transverse offset or angular misalignment [14]. Of these defects, transverse offset and angular misalignment are more important since splices are highly tolerant for longitudinal separation [8]. In terms of the two spot sizes, both splice losses due to transverse offset, α_d and due to angular offset, α_θ, can be obtained as [6]:

$$\alpha_d(dB)=4.343\left(d/W_p\right)^2, \tag{10}$$

$$\alpha_\theta(dB)=4.343\left(\pi n_2W_{rms}/\lambda\right)^2\theta^2, \tag{11}$$

where d is the transverse offset, θ is the angular offset.

2.4.2 Bend loss

Optical fibers suffer radiation losses at bends or curves on their paths. This is due to the energy in the evanescent field at the bend exceeding the velocity of light in the cladding, and hence the guidance mechanism is inhi-

bited, which causes light energy to be radiated from the fiber. Unlike splice and microbending losses, pure bend loss is not expressible in terms of either of the spot sizes. It depends on the propagation constant through the eigen functions U and W (3), (5). For an arbitrary index profile, the bend loss can be modeled as [9]:

$$\alpha_b(\mathrm{dB/m}) = A\sqrt{\frac{\pi V^8}{16aR_c W^3}}\exp\left\{\frac{-4R_c W^3\Delta}{3aV^2}\right\}, \qquad (12)$$

where R_c is the bend radius and A is a parameter depending on the modal field, F(R), and the index profile, f(R), and is defined as [9]:

$$A = \frac{\left(\int_0^\infty [1-f(R)]RF(R)dR\right)^2}{\int_0^\infty RF^2(R)dR}. \qquad (13)$$

(12) is based on an approximate model consisting of a current-carrying antenna of an infinitesimal thickness which radiates in an infinite medium of index equal to the cladding index. The approximation assumes that the equivalent core current of the bent fiber is superposed onto its axis. So, it ignores the effect due to the finite core cross- section. The correct form of the bend α_b is obtained by multiolying (12) by an area factor Γ given by [9]:

$$\Gamma = \int_0^\infty [1-f(R)]RF(R)I_0(WR)dR \Big/ \int_0^\infty [1-f(R)]RF(R)dR \qquad (14)$$

where I_0 is the zero order modified Bessel function of the first kind.

2.4.3 Microbending loss

When the fiber has a large number of random bends of arbitrary curvatures and lengths, the radiation is uncorrelated [10]. So, one can add the power losses from transitions and from bends. Thus the total microbending loss along the length of the fiber is the sum of the power radiated from each bend and from each transition. Provided that the ratio of bend to core radii is large, one can use the expression derived for bend loss. Microbending losss, α_{mic}, can also be calculated as a function of the spot sizes. Petermann has approximated it in the form [15]:

$$\alpha_{mic}(\mathrm{dB/m}) = (4.343/8)\left(K_0 n_1 w_{02}\right)^2 \Phi_p\left(2/K_0 n_1 w_{01}^2\right). \qquad (15)$$

where w_{01} and w_{02} are two auxiliary spot sizes which can be approximated from the following formulae, with a worst error less than 2% [15]:

$$w_{01}/W_p = 1 + 2.41(\zeta_0 - 1) - 0.93(\zeta_0 - 1)^2, \qquad (16)$$

$$w_{02}/W_p = 0.99 + 0.57(\zeta_0 - 1) - 0.37(\zeta_0 - 1) \qquad (17)$$

where $\zeta_0 = W_m/W_p$ and Φ_p is the curvature power spectrum, given by [15]:

$$\Phi_p(\Omega) = \Omega^4\sqrt{\pi}\sigma^2 L_c \exp\left(-0.5L_c^2\Omega^2\right), \qquad (18)$$

where σ is the rms deformation amplitude and L_c is the correlation length.

2.5 Chromatic dispersion

Intramodal or chromatic dispersion occurs in all fiber types and results from the finite spectral width of the optical source wich causes broadening of each transmitted pulse. Intramodal dispersion may be caused by two dispersive effects. The first is the material dispersion which depends only on the fiber material and how the refractive index vary with the operating wavelength. The second is the'waveguide dispersion which depends on the propagation constant and results from the variation of the group velocity for a particular mode. The waveguide dispersion can be neglected in multimode fibers but it is significant in single-mode ones [14].

In the present study, it is considered that the material of the cladding is pure silica and that of the core is a certain composition of GeO_2 and SiO_2 glasses. The refractive index of such system is represented by Sellmeier as [16]:

$$n^2 - 1 = \sum_{i=1}^{3}\frac{\left[SA_i + x(GA_i - SA_i)\right]\lambda^2}{\lambda^2 - \left[SL_i + x(GL_i - SL_i)\right]^2}, \qquad (19)$$

where x is the mole fraction of GeO_2 in the silica glass, and A_i are constants related to the number of particles in the material that can oscillate at wavelengths $L_i \cdot A_i$ and L_i are called Sellmeier coefficients. S denotes Silica and G denotes Germania glasses.

The total Intramodal (chromatic) dispersion of pulses bounded in a single-mode fiber is given as follows [17]:

$$D_T = (1/c)dN_T/d\lambda, \qquad (20)$$

where

$$N_T = (1/n_c)\left\{n_2N_2 + (0.5V\mathrm{db}/dV + b)(n_1N_1 - n_2N_2)\right\}. \qquad (21)$$

where n_c is the effective refractive index of the fiber, N_1 and N_2 are the group indices of the core and cladding, respectively.

The quantity (V db/dV) is expressed in terms of W, for any refractive index profile as [6]:

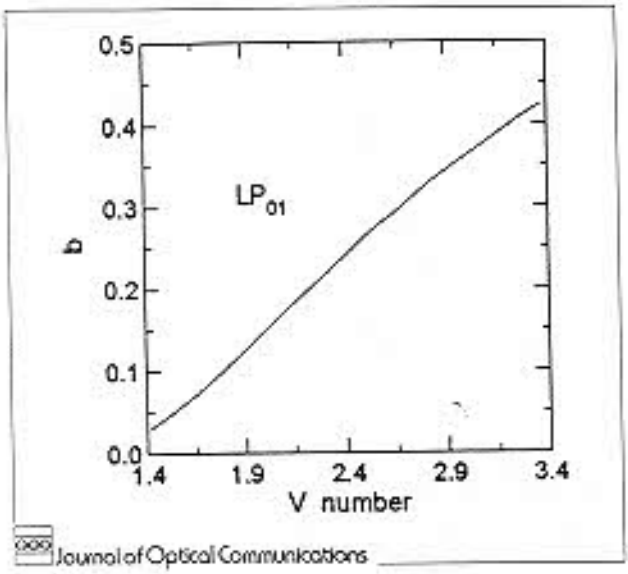

Fig. 1: The normalized propagation constant, b, of the fundamental mode in a graded index fiber as a function of the normalized frequency V

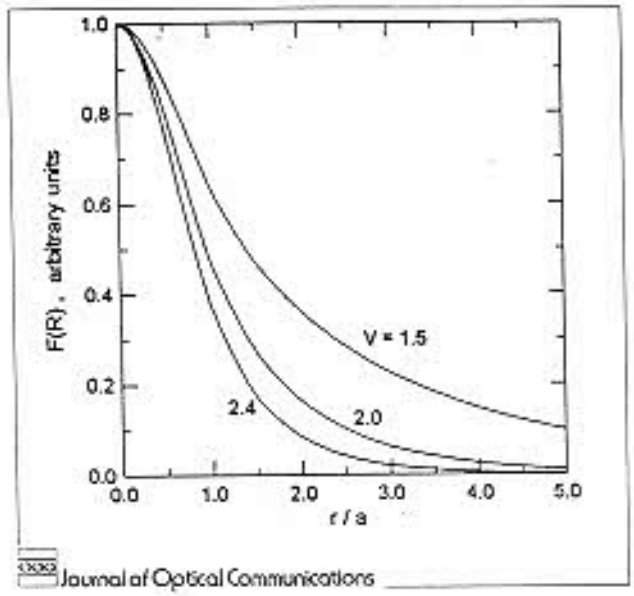

Fig. 2: Field distribution in the core ($r/a < 1$) and cladding ($r/a \geq 1$) for the fundamental mode

$$V\frac{db}{dV} = \frac{4a^2}{V^2 W_p^2}. \qquad (22)$$

Solving the above equations, one can get total dispersion coefficient D_T based on W_p.

3 Results and discussion

The normalized propagation constant, b, is obtained by solving the characteristic equation, (6), using an iteration technique with a worst error less than 2 %. Figure 1 represents the dependence of b on the V number. This dependence is fitted to an approximate relation as:

$$b = 0.371 - 0.869V + 0.641V^2 - 0.159V^3 + 0.014V^4. \qquad (23)$$

The procedure of determining the two spot sizes, W_{rms} and W_p starts with finding the electric field distribution in both core and cladding depending on the obtained propagation constant. Figure 2 represents (4a), (4b) which are the solutions of the wave equation for a parabolic profile. The electric field is displayed at values of V corresponding to single-mode operation. As expected, at higher values of V (near cutoff), it is noted that the fraction of the power launched in the core is high compared with that at lower values of V.

The two spot sizes W_p and W_{rms} are then calculated numerically for different fiber parameters, from (8), (9) using a computer code. Figure 3 shows a sample of results for both spot sizes at $\lambda = 1.3$ μm. It is noted that, at a certain value of core radius the W_{rms} spot size is generally high at lower values of Δ or equivalently at lower values of the V number.

The accuracy of the Kummer function solution is tested by comparing with the power series solution, (7), (8).

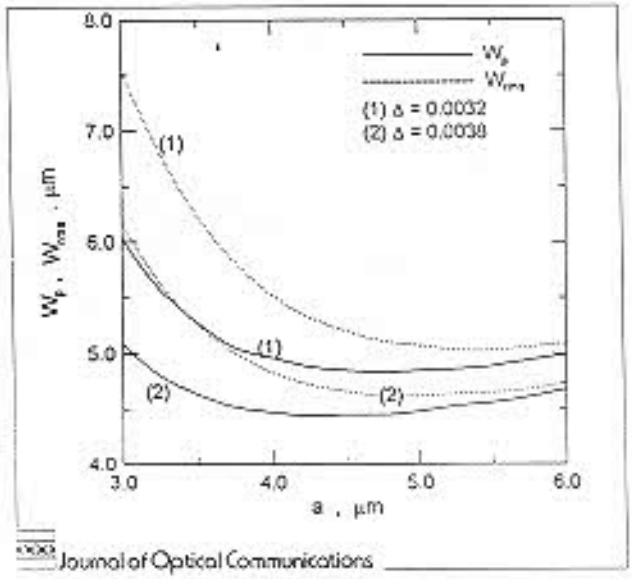

Fig. 3: Spot sizes W_p and W_{rms} as functions of the core radius a at $\lambda = 1.3$ μm

A fair agreement is noticed in Tables 1 and 2 which show this comparison for the normalized propagation constant, b, and the two spot sizes at different values of V.

Depending on the calculated values of both spot sizes, and the procedure explained in Sec. 2, the transmission characteristics are obtained and displayed in Figs. 4–8 in the 1.3 μm and 1.55 μm wavelength windows.

Figure 4 displays the splice loss due to transverse offset, α_d, as a function of core radius, a. The transverse offset, d, is taken equal to 1.0 μm [6, 14]. The dependence of α_d on both a and V be interpreted in the same manner as done for W_p, since α_d is inversely proportional to $(W_p)^2$, (10).

The splice loss due to angular offset, α_θ, is plotted against the core radius at the same operating wavelengths

Table 1: Comparison of rms and Petermann spot sizes for different graded index fibers with $\Delta = 0.0035$ operating at $\lambda = 1.3$ μm

a (μm)	V	Kummer Function Solution			Power Series Solution		
		b	W_{rms} (μm)	W_p (μm)	b	W_{rms} (μm)	W_p(μm)
3	1.761	0.090	6.89	5.54	0.092	6.83	5.51
4	2.348	0.225	5.14	4.68	0.230	5.13	4.69
5	2.935	0.347	4.81	4.63	0.350	4.82	4.65

Table 2: Comparison of rms and Petermann spot sizes for different graded index fibers with $\Delta = 0.0035$ operating at $\lambda = 1.55$ μm

a(μm)	V	Kummer Function Solution			Power Series Solution		
		b	W_{rms} (μm)	W_p(μm)	b	W_{rms} (μm)	W_p(μm)
3	1.477	0.037	10.2	8.40	0.040	10.13	8.27
4	1.969	0.137	7.12	6.01	0.140	7.08	6.00
5	2.461	0.252	5.98	5.53	0.254	5.98	5.55

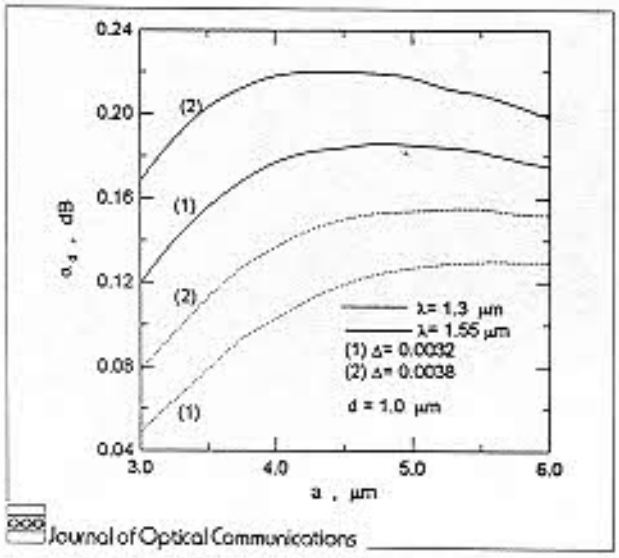

Fig. 4: Transverse offset loss α_a as a function of the core radius a

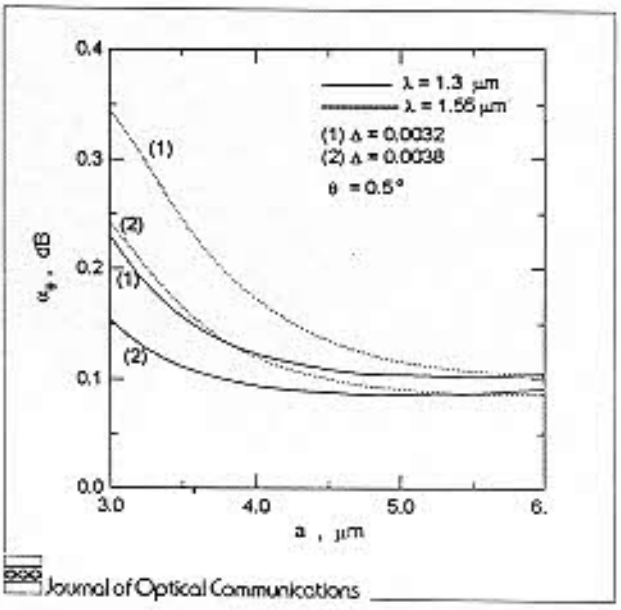

Fig. 5: Angular offset loss α_θ as a function of the core radius a

in Fig. 5. The angular offset, θ, is assumed to be 0.5° as typical offset at a fiber joint [6]. The splice loss, α_θ, shows the same dependence on both the core radius and the V number as W_{rms}, because of the direct proportionality between them, (11). It is noted that, operating at higher values of V increases the fraction of power transmitted in the core and decreases the splice loss due to angular offset to a minimum value. However, it causes the splice loss due to transverse offset to be very large.

Using (12) and (13), the bend loss, α_b, is evaluated and the results are plotted against the core radius at the same wavelength windows in Fig. 6.

Bend loss is calculated taking a bend radius of 1.25 cm and using the previously obtained modal field distribution. Bend loss is, generally, high at lower values of core radius, a, and then decreases with increasing a. This is because at lower values of a, the bend radius is near to the critical bend radius at which all transmitted power is lost through radiation. In consistence with results of step index fibers [6], the bend loss is of the same order of magnitude, and fibers exhibiting higher values of Δ have decreased sensitivity to macrobend loss as shown in Fig. 6.

Microbending loss is calculated from (15)–(18) and its variation with the core radius is shown in Fig. 7 for different values of Δ. For the curvature power spectrum given by (18) in estimating these microbend losses, a correlation length L_c of 300 μm and a value of 0.002 μm for the rms deformation amplitude, σ, were assumed on the basis of laboratory cable test as quoted by [4]. From Fig. 7, it is clear that microbending loss increases with core radius and becomes maximum at certain point, then it decreases. The maximum value of α_{mic} is sensitive to the value of the grading parameter Δ. As an example, the maximum value of α_{mic} increases from 0.035 to 1.33 dB/km when Δ increases from 0.0032 to 0.0038. Figure 7 assures that operation far from cutoff will decrease the microbending losses. This operation can be achieved either by decreasing the core radius, decreasing the grading parameter, or by operating at a higher wavelength window.

In studying dispersion, a core having a germania mole fraction of 3% and a pure silica cladding are utilized, which represent an actual fiber [16]. Figure 8 shows the variation of the chromatic dispersion coefficient, D_T, (20), with the operating wavelength, λ, for three fibers with different core radii. The obtained values of the zero-dispersion wavelength, λ_0, are respectively 1.34, 1.23, and 1.155 μm.

The dependence of the chromatic dispersion on both core radius and the operating wavelength shows nearly the same slopes for different values of core radius, but with different magnitudes. Since chromatic dispersion, D_T, is the algebraic sum of the material dispersion and the waveguide dispersion, so, the obtained results can be explained as follows:

The material dispersion determines the shape of the curves which is nearly the same for different core radii, while the waveguide dispersion affects the values of both D_T and λ_0, depending on the value of the core radius, a.

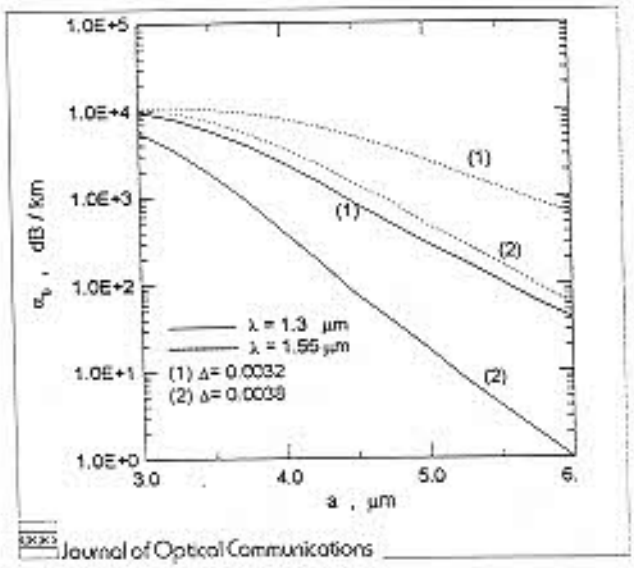

Fig. 6: Bending loss α_b as a function of the core radius a

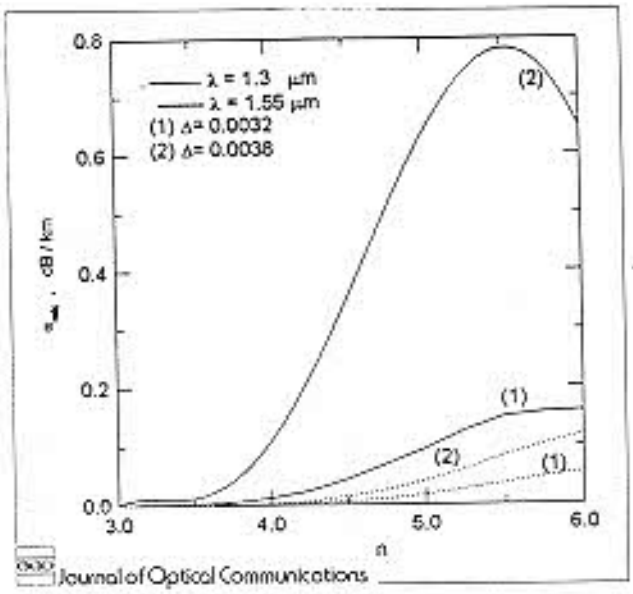

Fig. 7: Microbending loss α_{mic} as a function of the core radius a

Similar behavior is also obtained for other compositions with different values of x.

4 Conclusion

A detailed study for the transmission characteristics of single-mode graded index fibers, based on spot size calculations, is presented. Results at 1.3 µm and 1.55 µm wavelength windows have been shown in a series of graphs. At a certain value of the core radius, both values of spot sizes W_p and W_{rms} are generally high at lower values of Δ or equivalently at lower values of the V number. The dependence of the transverse splice loss, α_t, and the angular splice loss, α_θ, on both core radius and the V number could be interpreted in the same manner as done, respectively, for W_p and W_{rms}. It has been found that both bending loss, α_b, and microbending loss, α_{mic}, increase with the core radius. The results also show that α_θ decreases and both α_t and α_{mic} increase with the operating wavelength while α_b is negligibly affected. The study of the chromatic dispersion assures that the waveguide dispersion component affects the value of the dispersion coefficient and shifts the zero material dispersion wavelength to lower values at greater core radii.

This study is useful as a general guideline for system designers concerned with best designs of single-mode fiber systems.

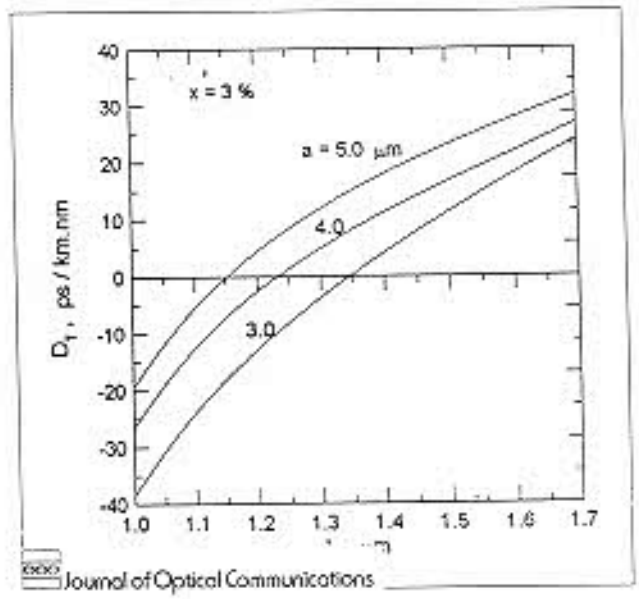

Fig. 8: Chromatic dispersion coefficient D_T as a function of the operating wavelength λ

References

[1] Shih-Chieh Chao: "Extended Gaussian Approximation for Single Mode Graded Index Fibers"; IEEE J. Lightwave Technol. LT-12 (1994) 3, 392–395

[2] D. Marcuse: "Low Dispersion Single-Mode Fiber Transmission – The Question of Practical versus Theoretical Transmission Bandwidth"; IEEE J. Quantum Electron QE-17 (1981) 6, 869–877

[3] David N. Payne: "Development of Low – and High – Birefringence Optical Fibers"; IEEE J. Quantum Electron. QE-18 (1982) 4, 477–487

[4] B. P. Pal; Vishnu Priye; Ramanand Tewari, K. Thyagarajan: "Estimation of Spot Sizes from the Far-Field Measurement of a Single-Mode Fiber"; J. Opt. Commun. 10 (1989) 2, 70–73

[5] W.T. Anderson, V. Shah: "Mode-Field Diameter Measurements for Single-Mode Fibers with Non-Gaussian Field Profiles"; IEEE J. Lightwave Technol. LT-5 (1987) 2, 211–216

[6] B. P. Pal; U. K. Das; N. Sharma: "Effect of Variation in Cutoff Wavelength on the Performance of Single-Mode Fiber Transmission in the 1300 nm and 1550 nm Wavelength Windows"; J. Opt. Commun. 10 (1989) 3, 108–114

[7] M. Abramowitz; I. A. Stegun: "Handbook of Mathematical Functions"; New York, Dover publications, 1965

[8] Akihiko Ishikura: "Loss Estimation in Mass Splicing of Single-Mode Fiber Ribbons"; J. Opt. Commun. 10 (1989) 2, 56–60

[9] Allan W. Snyder, John D. Love: "Optical Waveguide Theory" New York, Chapman and Hall Ltd., 1983

[10] Clemens Unger: "Investigation of the Microbending Sensitivity of Fibers"; IEEE J. Lightwave Technol. LT-12 (1994) 4, 591–596

[11] Klaus Petermann: "Upper and Lower Limits for the Microbending Loss in Arbitrary Single-Mode Fibers"; IEEE J. Lightwave Technol. LT-4 (1986) 1, 2–6

[12] F. Gauthier, J. Auge: "Consistent Refractive Index Profile Measurements of a Step Index Monomode Fiber Attained by Several Techniques"; IEEE J. Quantum Electron QE-17 (1981) 6, 885–889

[13] W. Streifer: "Scalar Analysis of Radially Inhomogeneous Guiding Media"; J. Opt. Soc. Am. 57 (1967) 1, 779–786

[14] John M. Senior: "Optical Fiber Communications: Principles and Practice"; London, Prinice Hall International Ltd. 1992

[15] S. B. Andereasen: "Combined Numerical and Analytical Method of Calculating Microbending Losses in Single-Mode Fibers with Arbitrary Index Profiles"; IEEE J. Lightwave Technol. LT-4 (1986) 6, 596–600

[16] J. W. Fleming: "Dispersion in GeO_2 – SiO_2 Glasses"; Appl. Opt. 23 (1984) 24, 4486–4493

[17] Paulo S. M. Pires: "Prediction of Laser Wavelength for Minimum Total Dispersion in Single-Mode Step Index Fibers"; IEEE Trans. Microwave Theory Tech. MTT-30 (1982) 2, 131–140